International Journal of Power Electronics and Drive System (IJPEDS)
Vol. 8, No. 4, December 2017, pp. 1793~1803
ISSN: 2088-8694, DOI: 10.11591/ijpeds.v8i4.pp1793-1803

Fault Detection & Classification in UPFC Integrated Transmission Line Using DWT

S.K Mishra[1], S.C Swain[2], L.N Tripathy[3]
[1,2]Department of Electrical Engineering, KIIT University
[3]Department of Electrical Engineering, BijuPatnaik University of Technology

Article Info

Article history:

Received Sep 17, 2017
Revised Nov 14, 2017
Accepted Dec 1, 2017

Keyword:

Fault Inception Angle (FIA)
Fault resistance (Rf)
Single-circuit line
Source Impedance (SI)
Spectral Energy (SE)
Threshold (Th)

ABSTRACT

Fault detection and classification in UPFC (Unified Power Flow Controller) integrated transmission line using single terminal based DWT (Discrete Wavelet Transform) is proposed. The current is extracted from the sending end bus and processed through wavelet transform to evaluate the spectral energy (SE) using db4 mother wavelet. Three level decomposition is framed to extract the fundamental frequency component from non-stationary signal, considering sampling frequency of 2kHz system. The fundamental frequency component of respective phase currents are used to compute SE at sending end. The SE of individual phase current is the key factor for deciding the fault pattern detection and classification. The advantage of using this it requires less cost and protect entire transmission line with minimal fault detection time. The various types of fault (L-G, L-L, L-L-G, L-L-L) are simulated by considering the parameter like fault resistance, source impedance, fault inception angle, multi-location fault, reverse power flow and UPFC system parameter. The scheme works reliable and efficient to detect and classify the fault within a cycle of time period 20ms.

Corresponding Author:

S K Mishra,
Departement of Electrical Engineering,
KIIT University,
Kathajodi campus, Patia, Bhubaneswar, India.
Email: mishra29y@yahoo.com

1. INTRODUCTION

Transmission line integrated FACTS [1] (flexible AC transmission system) controllers are the emerging research in the field of power system protection. Now-a-days, FACTs [2] devices are integrated increasingly to the transmission line across many parts of the world. The most versatile FACTs controller device prevailing at present is the combination of both shunt and series controller device known as UPFC [3] (unified power flow controller). Not only it provides independent control parameter like active power, reactive power, impedance and voltage of transmission line but also enhances the transmission capacity of the line. It comprises of two linked self-commutating converters through both series and shunt transformers integrated to the line. UPFC [4] exists in the fault loop affects to some extent to voltage and current at the relaying point. This relay depicts the detail regarding fault detection and classification of the transmission line.

The process of fault detection thereafter tripping signal issue to CB (circuit breaker) are to be coordinated in a well manner suitable using DWT based approach to detect fault pattern classification. The fault occurs in the transmission line includes, L–G (line–to-ground), L–L (line–to-line), LL–G (double line–to-ground) and L-L-L(triple line) and produces error in the measurement of conventional relaying scheme which can be overcome by applying digital relays. Conventional relaying scheme like distance relay [5] used for fault detection and classification based on the measurement of power frequency and lacks owing to the

fault resistance, mutual coupling between the adjacent lines, location of fault, influence of reactance. To overcome conventional method, new approach is adopted to provide better accuracy and reliable operation. Digital relay operation based relaying is also possible in double circuit transmission line based on travelling wave [6] theory the problem in this is large expanse of hardware setup is needed to trip the signal. As the travelling wave contains high frequency signals, it is very difficult to separate the frequency components from interference as well as noise. Neural network based ANN [7] including fuzzy logic approach is also discussed in [8]. Fuzzy logic approach individually requires more computational time to analyse during the fault as it is sensitive to frequency changes. ANN based approach based on highly training and testing process is possible to analyse the fault. However during the process some neurons are missed due to phasor data computation which produces inaccurate result. In addition to that it requires more processing time compared to other approach.

Ultra high speed relay for EHV/UHV transmission lines also discussed in [9] for different fault classification in the transmission line. Researchers have been identifying many new types of approach for faulty zone detection and classification. One of the approach in the field of protection is Kalman filtering discussed in [10], the problem in this is the requirement of a number of dissimilar filters. Another promising hybrid approach of machine intelligence and support vector machine (SVM) also discussed in [12] for fault identification and classification, but it is more prone to noise and interferences. In addition to this it provides result with higher inaccuracy when signal-to-noise ratio is considered for 30 db [11]. Fault identification using linear time-frequency distribution for VSI switch is discussed in [12], however it fails to explain fault detection time of different fault considered and its relay response time. In detection and classification of faults in matrix converter [13] also explains open circuit and short circuit fault of switching component but unable to detect and classify shunt fault occurred in transmission line propoerly. Fault current limiter [14] circuit explains to improve transient stability, but it unable to trace different shunt faults condition except short circuit fault.

Classification of fault using wavelet multi-resolution analysis and neural network is also discussed in [15], however db4 wavelet at six level decomposition methods are discussed which require more processing time compared to proposed work of third level decomposition in addition to this it unable to explain fault detection time and proper classification of fault including system parameter change. In Adaline LMS control and DWT approach [16] based STATCOM integrated line explains the power quality improvement in adaptive linear neural network and DWT approach used for fault detection and classification but it unable to explain the fault detection time properly. Though fault detection and classification is explained in SVC integrated double circuit line using FDST [17] but fails to address the fault detection time. The decision tree [18] approach requires more processing time due to its burden. All these approach based detection and classification scheme are outlined excluding UPFC integrated line. However the transmission line integrated to UPFC then the scheme becomes very complex to analyse the fault. Therefore a strong motivation behind the scheme is to develop an algorithm which provides fast detection time or relay response time to process.

This paper comprises five different section including introduction part in section-1. Section-2 discusses DWT based Signal Processing technique relaying scheme. Section-3 discusses studied system and explains proposed methodology effectively for evaluating fault detection and classification. Section-4 describes the discussion of simulation result considering the effect of parameter change. Section-5 explains conclusion part of proposed scheme.

2. SIGNAL PROCESSING TECHNIQUE

The Signal processing tool have been used for evaluation of fault detection and classification. Out of many numerous tool used in power system protection, wavelet transform [19],[20] is considered to be a powerful tool for processing highly non-stationary signal containing different high order harmonics. To evaluate fundamental signal from the transient non-stationary signal occured during the fault analysis of window size is an impoertant issue to discuss which splits into number of adjustable size region according to its frequency. Therefore the accuracy becomes more and more with low-frequency data using longer time intervals whereas high-frequency data using shorter time interval. DWT offers time-frequency transformation rather than time-scale region. Further it is also used to decompose signal into a set of basic functions known as wavelets. Mother wavelet [21] of Daubechy's group db4 is decomposed into various scaled and shifted forms to achieve prototype wavelets. Selection of suitable mother wavelet Daubechy family [22] is considered to be best because its accuracy is higher compared to other type of mother wavelet. Number of filters like high pass (H.P) and low-pass (L.P) filters are used to obtain fundamental component of current discussed in Mallat's algorithm [20]. MRA approach of wavelet provides fast and short transients disturbances which is detected at lower scales. As discussed db4 [21], [22] performs well as compared to other type of mother wavelet.The Signal processing tool have been used for evaluation fault detection and

classification accurately. Out of many tool used in power system protection, wavelet transform [19],[20] is considered to be the one of the powerful tool for processing highly non-stationary signal containing different higher order harmonics. The window size can be streched into number of adjustable size region according to its frequency range. Therefore the accuracy becomes more with low-frequency data using longer time intervals whereas high-frequency data can be found using shorter time interval window. DWT offers time-frequency transformation rather than time-scale region. Further it also used to decompose signal into a set of basic functions known as wavelets. Mother wavelet [21] of Daubechy's group db4 is decomposed into various scaled and shifted forms to achieve prototype wavelets. Selection of mother wavelet [22] is considered here for its higher accuracy compared to other type of mother wavelet. Number of filterslike high pass (H.P) and low-pass (L.P) filters used to obtain fundamental component of current discussed in Mallat's algorithm [20]. MRA approach used for fast and short transients disturbances are detected at lower scales. CWT signal x (t) is expressed as

$$CWT(a,b) = \frac{1}{\sqrt{a}} \int_{-\infty}^{+\infty} x(t)\, \varphi \frac{(t-b)}{a}\, dt \quad (1)$$

Where, $\varphi_{a,b}(t) = \varphi \frac{(t-b)}{a}$ is known as mother wavelet; 'a' and 'b' are two parameters known as dilation and translation parameter.

DWT converts time signal to wavelet signal in discrete form and transforms into input series of HP (H_i) and LP (G_i) coefficients x_0, x_1,…..x_n (length n/2 each). This is expressed by

$$H_i = \sum_{n=0}^{s-1} x_{2j-n} \times u_n(z) \quad (2)$$

$$G_i = \sum_{n=0}^{s-1} x_{2j-n} \times v_n(z) \quad (3)$$

Where, $u_n(z)$ and $v_n(z)$ are known as wavelet filters and ***s*** is known to be filter length, j=0, ... [n/2]-1.

The process starts with the extraction of individual current signal of phase (A, B, C) at sending end of the transmission line. The scheme has been considered for 2 kHz sampling frequency (40 samples per cycle in 50 Hz system) for the simulation study. Signal decomposition is performed by considering three decomposition level. First level decomposition, a1 of 0–1kHz, d1 of 1–2 kHz, second level decomposition, a2 of 0–500Hz, d2 of 500Hz–1kHz and third level decomposition a3 of 0–250Hz, d3 of 250–500Hz respectively. So, third level decomposition of a3 has fundamental component of frequency (50 Hz), 3rd harmonics and 5th harmonics component of current. In the 3rdlevel, the reconstructed current signal of respective phase current (A3) from the approximate coefficient (a3) obtained at sending end terminal. From this reconstructed current signal r.m.s values of fundamental current signals are extracted. The current signal using DFT is used for computation of Spectral Energy [23].

3. STUDIED SYSTEM

The studied model of two substation each of having capacity of 400 kV voltage, 50 Hz frequency and short circuit level 1500MVA between a transmission lines of 400km length depicted in Figure1(a). UPFC capacity of 100MVA is integrated at mid-point of line (Distributed model) and 48-pulse voltage source inverters (VSI) associated through two common DC capacitors of 2500µF.STATCOM and SSSC are shunt and series connected through transformer 15kV/400kV and 15kV/22kV which injects/consumes reactive power to/from transmission system to regulate active power and bus voltage. The UPFC modelling and controller design presented in the scheme is referred [24], [25]. Spectral Energy [26] based one terminal (sending end bus) is the key point for deciding the fault pattern and classification. The relaying theory based application is referred [27]. Figure 1(b) and Figure1(c) depicts the schematic diagram and flow chart of the scheme respectively. In the Figure 1(a) substation voltage of sending end and receiving end are considered as V_s and V_r respectively and δ (in degree) is phase angle difference between them. Mathematically, $V_S = Vr$ =400 kV, δ =δs – δr= 12^0- 0^0. Impedances Zs and Zr are considered for sending and receiving end. B_{se} and B_{re} are considered for sending end and receiving end bus. Transmission line is subdivided into four equal sub-sections of 100km line length having Z_{l1}, Z_{l2}, Z_{l3} *and* Z_{l4} respectively. Z_1= (0.01537Ω+j0.2783Ω)/km and Z_0= (0.04612Ω+j0.8341142Ω)/km are considered for positive and zero sequence impedance of the proposed transmission line.

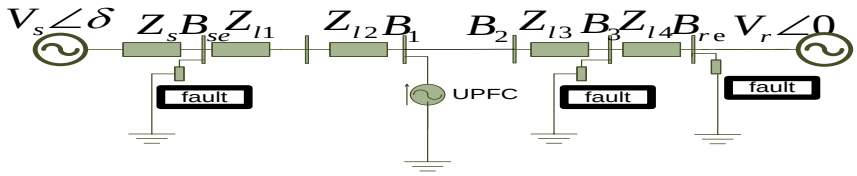

Figure 1(a). Proposed scheme of UPFC integrated transmission line

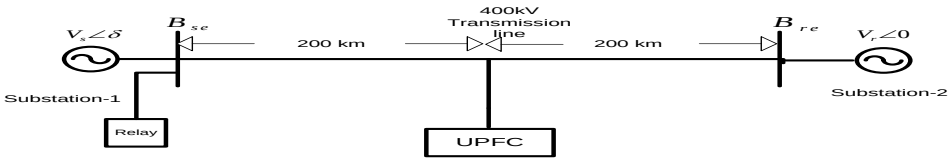

Figure 1(b). UPFC integrated at mid-point of transmission line length of 400km

The flow chart of proposed scheme is depicted in Figure 1(c). The different types of parameter variations are considered for the proposed scheme to study fault detection and classification which are mentioned below.

- Variation of Fault resistance (Rf): 0 to 100Ω.
- Variation of fault inception angle (FIA): 0^0,45^0,90^0.
- Variation of reverse power flow and normal power flow.
- Variation of source impedance (SI).
- Variation of UPFC parameter (Vse and θse).
- Series injected voltage variation (Vse varies from 0 to 10% of the normal voltage).
- Series injected voltage angle variation (θse varies from 30^0 to 120^0).
- Variation of fault distance at different location

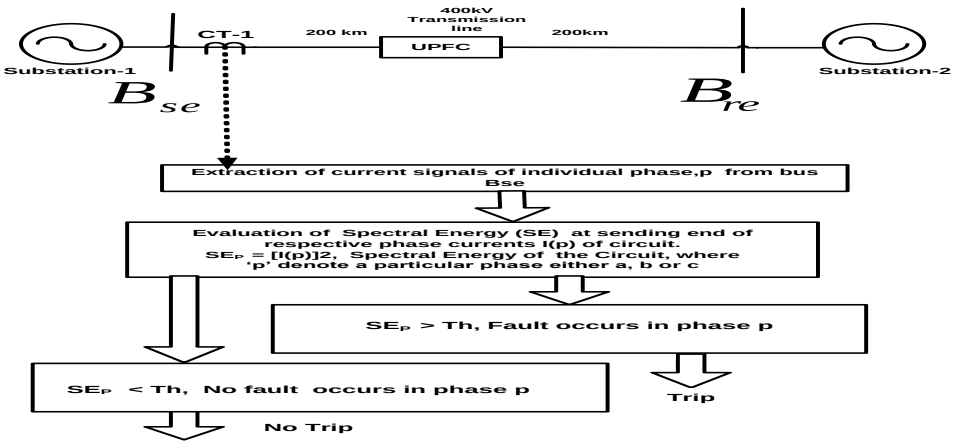

Figure 1(c). Flow chart of proposed scheme of UPFC integrated transmission line.

Spectral Energy (SE) of phase current at sending end of the line is evaluated from the fundamental component of current magnitude using DWT. The SEp (SE of p-phase) is computed by using equation (5).The SEP obtained at sending end are compared with the set threshold (Th) values for fault detection and classification purposes. 'R2010a' Matlab platform is used for simulation study by considering fault initiation time at 0.3 second (600th sample of sampling frequency equal to 2 kHz in 40 samples/cycle). The magnitude, phase angle of fundamental component current phase 'p' is extracted from DWT reconstructed current signal and is expressed by,

$$I(p) = |I(p)| \tan^{-1}\left(\frac{\mathrm{Im}\, I(p)}{\mathrm{Re}\, I(p)}\right) \quad (4)$$

where, $|I(p)|$ & $\tan^{-1}\left(\frac{\mathrm{Im}\, I(p)}{\mathrm{Re}\, I(p)}\right)$ are magnitude and phase angle of fundamental component of current of phase *p*. The SE_P of the current signals phase, *p* at sending end is given by

$$SE_P = |I(p)|^2 \quad (5)$$

The following mentioned case contributes information regarding detection and classification of fault. **Case1**:-$SE_P > Th$: The fault is within the circuit in p phase from sending end bus. **Case2**:-$SE_P < Th$: No fault occurs within the circuit in p phase from sending end bus. The threshold (*Th) is* carefully chosen as 25 for our test system, after conducting number of simulation for different fault types including wide parameter variation as well as UPFC parameters.

4. RESULT AND DISCUSSION

'Mat lab Simulink' is prepared to model the proposed scheme of UPFC integrated transmission line. Different shunt faults L-G, LL-G, L-L, L-L-L and LLL-G are considered for simulation study, incepted at 0.3 seconds. Figure 2(a) depicts fault current retrieved from sending bus (B_{se}) of A-G fault incepted at 0.3 second.

Table 1. Variation of Rf (1Ω -100Ω) at FIA=0^0, FDT (Fault detection time) and distance in km from B_{se}

Type of fault	Rf=1 Ω FDT, distance from B_{se}	Rf=50Ω FDT, distance from B_{se}	Rf=100Ω FDT, distance from B_{se}	Fault classification
A-G	9ms, 10km	9ms,10km	10ms,10km	A-phase
A-G	9ms,390km	9ms,390km	9ms,390km	A-phase
AB-G	19ms,200km	18ms,200km	19ms,200km	AB-phase
BC-G	18ms,10km	19ms,10km	19ms,10km	BC-phase
ABC	15ms,100km	16ms,100km	18ms,100km	ABC-phase

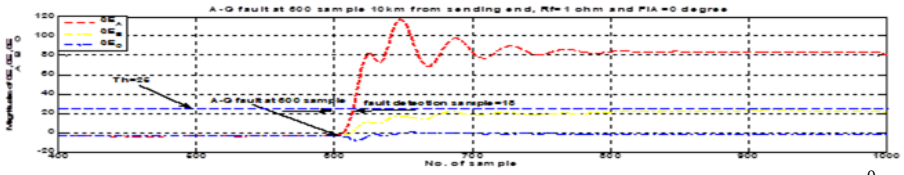

Figure 2(a). A-G fault at sending end (B_{se}), fault incepted at 600 sample Rf =1Ω, FIA=0^0.

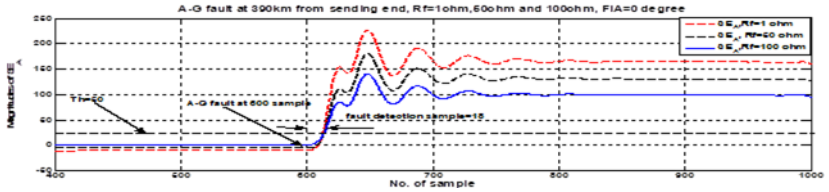

Figure 2(b). A-G fault at 390km distance from B_{se} at the Variation of Rf =1Ω, 50Ω and 100Ω, FIA=0^0 the Variation of Rf =1Ω, 50Ω and 100Ω, FIA=0^0

4.1. Variation of fault resistance (*Rf*):

The variation of *Rf* is an important parameter in the protection scheme. To test system performance as well as accuracy, *Rf* values are considered for variation from 1Ω to 100Ω. Figure 2(b) depicts BC-G fault occurs at 10km distance from B_{se} at *Rf*=1Ω and FIA=0^0. It shows that the spectral energy (SE) of fault current B and C grows higher and crosses the threshold, Th=25 and detects the fault at 36 sample (18ms) to issue the signal to trip circuit breaker. Therefore the fault is detected and classified as BC-G fault. Figure 2(c) depicts A-G fault occurs at 10km distance from B_{se} at *Rf*=1Ω and FIA=0^0. The figure shows that SE of A phase

current grows higher as compared to B and C phase and crosses Th=25 to detect the fault in 18 sample (9ms) and classify the fault as A phase fault. Figure 2(d) depicts A-G fault at 390km distance from B_{se} at *Rf*=1Ω, 50Ω and 100Ω, FIA=0^0. It is seen from the figure that in all the three different case of *Rf*, SE grow higher and crosses Th value to detect fault in 18 sample (9ms). The *Table1*.Shows the variation of *Rf*=1Ω, 50Ω and 100Ω, FDT (fault detection time) and distance in km from B_{se} respectively.The variation of *Rf* works fine under all different types of fault condition.

4.2. Variation *of Source Impedance (SI):*

The variation of *SI* is also an important point to study for the system to be strong or weak under different types of fault condition. The different fault conditions are tested for different values of *SI* such as*Normal SI (NSI), SI* is increased by 5% of *NSI*, 10%, 15%, 20%, 25% then to 30%. Figure-3 depicts A-G fault occurs at 200km distance from B_{se} at Rf=1Ω, FIA=0^0 and *SI*=0 to 30% increase of *NSI*, it shows that SE in all the case grows up word direction and crosses Th value and detects the fault in 18 sample (9ms).. *Table2.* Presents the variation of *SI* (5%, 10%,15%,20%,25% and 30% increase of *NSI*), FDT and distance in km from B_{se}.

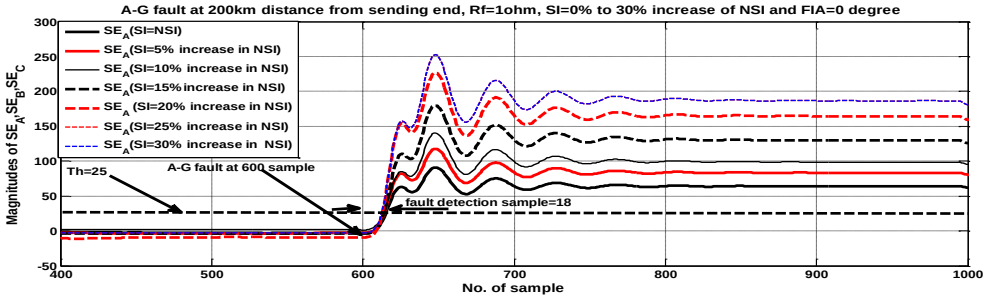

Figure 3. A-G fault at 200km distance from B_{se} at Rf =1Ω, SI=0% to 30% increase of NSI and FIA=0^0

Table 2. Variation of SI (5% to 30% increase of NSI) at Rf =1Ω, fault distance in km from B_{se}

Fault type	SI=5% +NSI, FDT, distance	SI=10% +NSI, FDT, distance	SI=15% +NSI, FDT, distance	SI=20% +NSI, FDT, distance	SI=25% +NSI, FDT, distance	SI=30%+NSI, FDT, distance
A-G	9ms,200km	9ms,200km	9ms,200km	9ms,200km	9ms,200km	9ms,200km
AB-G	18ms,300km	18ms,300km	18ms,300km	18ms,300km	18ms,300km	18ms,300km
CA	15ms,100km	15ms,100km	15ms,100km	15ms,100km	15ms,100km	15ms,100km
ABC	19ms,399km	18ms,399km	17ms,399km	18ms,399km	18ms,399km	19ms,399km

4.3. Variation of Fault Inception Angle (FIA):

The performance of *FIA*are also simulated by carrying out the number of simulations at *FIA* (30^0, 45^0 and 90^0). In Figure4, A-G fault occurs at 200km distance from B_{se} at Rf =1Ω and *FIA*=30^0,45^0 and 90^0 in all the case SE of A-phase crosses Th value and detects the fault sample 27 (13.5ms) and classify as A phase fault. Further it is seen that the *FIA* of lower value has higher magnitude compared to *FIA* of higher value. *Table3.*Shows thevariation of *FIA*, FDT and distance in km from B_{se} for different types of fault at Rf=1Ω, FIA (30^0,45^0 and90^0) respectively.

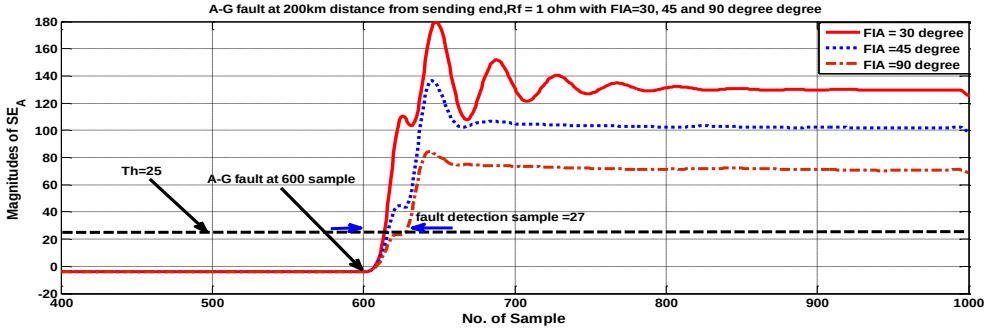

Figure4. A-G fault at 200km distance from B_{se} at Rf =1Ω, FIA=30^0, 45^0 and 90^0

Table 3. Variation of FIA (0^0, 30^0, 45^0 and 90^0) at Rf =1Ω, fault distance in km from B_{se}

Fault Type	FIA=0^0 FDT, distance	FIA=30^0 FDT, distance	FIA=45^0 FDT, distance	FIA=90^0 FDT, distance	classification
A-G	9ms, 200km	9ms,200km	9ms,200km	13.5ms,200km	A-phase
CA-G	16ms,100km	16ms,100km	16ms,100km	18ms,100km	CA phase
AB	15ms,300km	15ms,300km	15ms,200km	18ms,200km	AB phase
ABC	17ms,10km	17ms,10km	18ms,10km	19ms,200km	ABC phase

4.4. Variation of Normal power flow and phase reversal:

The phase reversal is critical issue while studying fault detection and classification under different types of fault in the power system protection. To validate proposed scheme, simulations are carried out to justify performance of the system. Figure 5 depicts C-G fault at 200km distance from B_{se} at Rf=1Ω, FIA= 0^0 with phase reversal. A comparative study is presented between normal power flow and reverse power flow. In case of normal flow of power angle, δ_1 =12^0 and δ_2= 0^0, on the other hand in reverse flow of power, δ_1=0^0 and δ_2=12^0 are considered for phase reversal simulation. From these waveform it is clearly noticed that, SE of C-phase grows in up word direction and crosses Th value to detects the fault where as the FDT takes 27 sample (13.5ms) in reverse power flow and FDT is reduced to 18 sample (9ms) in normal power flow. Thus the C-phase fault is clearly detected and classified both in normal and reverse power flow. *Table4.* Presents variation of phase reversal and normal power flow, FDT and distance in km from B_{se}.

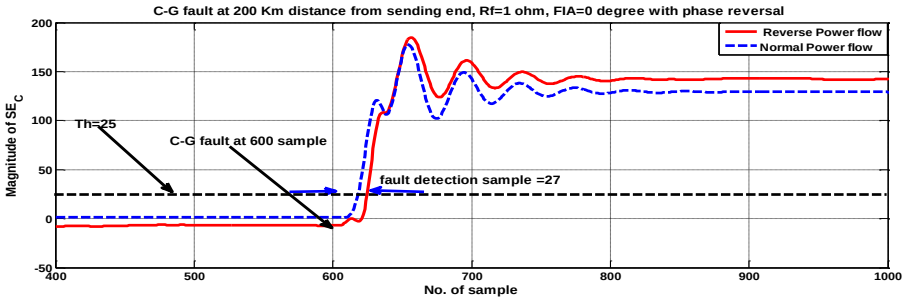

Figure 5. C-G fault at 200km distance from B_{se} at Rf =1Ω, FIA=$0^0$with phase reversal

Table 4. Phase reversal and normal power flow at Rf =1Ω, FIA=0^0, fault distance in km from B_{se}

Fault Type	Normal power flow FDT, distance	Reverse power flow FDT, distance	classification
C-G	10ms, 200km	13.5ms, 200km	C-phase
AB-G	12ms,100km	15ms,100km	AB-phase
BC	17ms,10km	19ms,10km	BC-phase
ABC	16ms,300km	19ms,300km	ABC-phase

4.5. Variation of UPFC operating condition:

UPFC variation such as series injected voltage, V_{se} as well as series injected voltage phase variation, θ_{se} are also an important parameter to study. It has significant impact in relation to performance of proposed scheme. Figure 6(a) depicts C-G fault at 200km distance from sending end, Rf=50Ω at V_{se} = 5%,10% and 15% increase of V_{se} in all the three case the SE increases in up word direction and crosses Th value, and the fault is detected within 27 sample (13.5ms). Further it is seen that the magnitude of SE reduces as the V_{se} value reduces. *Table-5* presents V_{se} variation of UPFC (5%, 10% and 15% increase of V_{se}), FDT and distance in km from B_{se}. Figure 6(b) depicts C-G fault at 200km distance from B_{se} at Rf =1Ω, θ_{se} of UPFC injected voltage (30^0 and 120^0), it is seen that the θ_{se} =30^0 takes less sample as compared to θ_{se} =120^0 and fault is detected in 18 sample and 27sample (9ms and 13.5ms) respectively and classified as C-phase fault. *Table 6.* Presents θ_{se} of UPFC injected voltage (30^0, 60^0 and 120^0), FDT, distance in km from B_{se}.

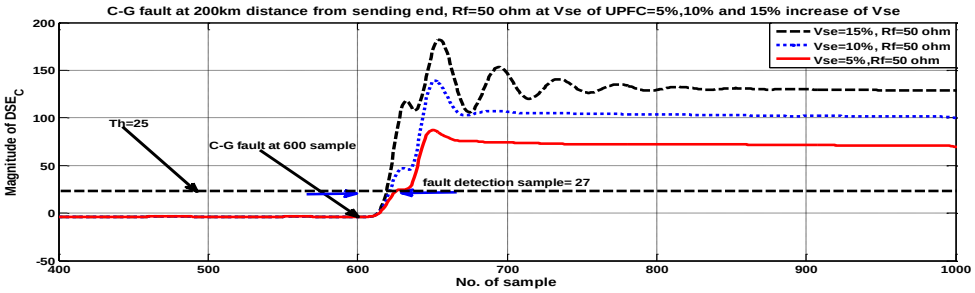

Figure 6(a). C-G fault at 200km distance from B_{se} at Rf =50Ω, V_{se} of UPFC= 5%, 10% and 15% increase of V_{se}

Table 5. V_{se} of UPFC (5%, 10% and 15% increase of V_{se}) at Rf =50Ω, fault distance in km from B_{se}

Fault Type	V_{se} =5% FTD, distance	V_{se} =10% FTD, distance	V_{se} =15% FTD, distance	Classification
A-G	13.5ms, 200km	10ms, 200km	10ms,200km	A-phase
CA-G	16ms,100km	14ms,100km	14ms,100km	CA-phase
AB	18ms,300km	16ms,300km	16ms,300km	AB-phase
ABC	19ms,399km	16ms,399km	16ms,399km	ABC phase

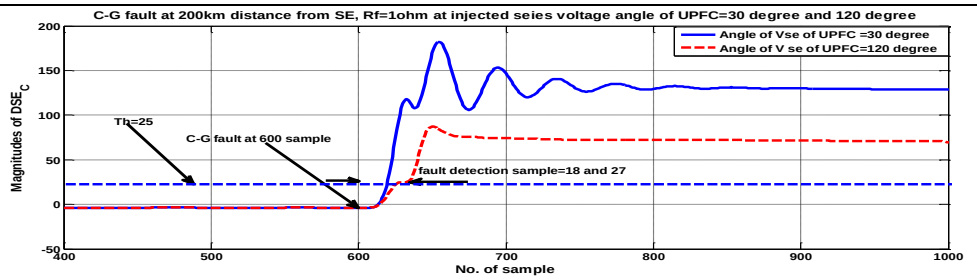

Figure 6(b). C-G fault at 200km distance from B_{se} at Rf =1Ω, θ_{se} of UPFC injected voltage (30^0 and 120^0)

Table 6. UPFC injected angle at Rf=1Ω, θ_{se} =30^0, 60^0 and 120^0, fault distance in km from B_{se}

Fault Type	θ_{se} =30^0 FDT, distance	θ_{se}=120^0 FDT, distance	Classification
C-G	9ms, 200km	13.5ms, 200km	C-phase
AB-G	12ms,100km	15ms,100km	AB-phase
BC	15ms,399km	18ms,399km	BC-phase
ABC	16ms,1km	18ms,1km	ABC-phase

4.6. Variation of fault distance at different location of UPFC:

Different fault location of UPFC in B-phase fault 100km, 200km and 300km distance from B_{se} are considered to justify the scheme accuracy depicted in Figure7. It is seen that the FDT in all three case are same as 9ms, irrespective of fault distance to detect and classify the fault. Very often this FDT changes as the parameter of the scheme changes. The magnitude of B-phase fault in case of 100km distance is higher compared to the B-phase fault of 300km distance. *Table7.* Shows the variation of distance with respect to FDT in different types of fault. It is seen that in all the case FDT remains within a cycle period of time 20ms.

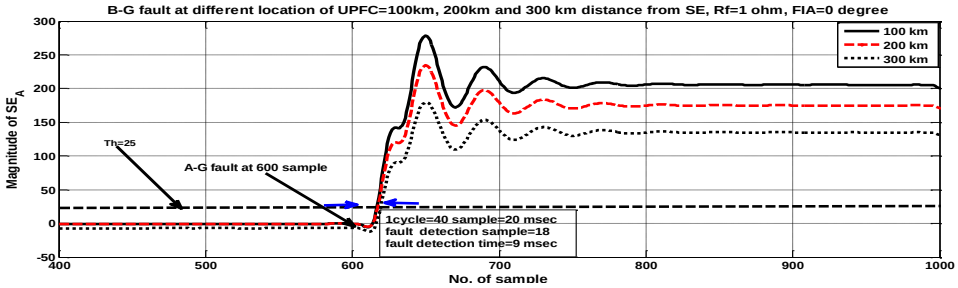

Figure7. B-G fault at different distance (100km, 200km and 300km) from B_{se} at Rf =1Ω, FIA=0^0

Table 7. Variation of UPFC at distance (100km, 200km and 300km) from B_{se}, Rf =1Ω and FIA=0^0

Fault Type	100km, FDT	200km, FDT	300km, FDT	Classification
B-G	9ms	9ms	9ms	B-phase
BC-G	12ms	12ms	15ms	BC-phase
BC	13ms	15ms	15ms	BC
ABC	15ms	17ms	17ms	ABC

Table 8. A comparison study of spectral energy of phase in different types of fault before and after UPFC

Fault type	Absolute entropy coefficients x 10^5 (before UPFC) [28]			Proposed scheme of Spectral Energy of phase (before UPFC)			Absolute entropy coefficients x 10^5 (after UPFC) [28]			Proposed scheme of Spectral Energy of phase (after UPFC)		
Phase	A	B	C	A	B	C	A	B	C	A	B	C
AG	**2.82**	1.92	1.83	**129.6**	14.87	3.41	1.95	1.52	2.09	**127**	13	10.5
BG	1.59	**2.52**	2.23	12.14	**113.9**	8.33	1.79	1.789	1.76	13.1	**112**	12.8
CG	1.98	1.58	**2.93**	13.67	10.4	**128.9**	1.51	1.81	2.11	13.4	12.9	**86.7**
AB	**9.98**	**8.57**	1.82	**127.9**	**114.4**	12.73	4.29	3.59	1.75	**85.2**	**135**	13.3
BC	1.56	**6.66**	**5.39**	12.28	**125.6**	**113.4**	1.51	3.49	3.042	12.8	**84.2**	**134**
CA	**9.83**	1.56	**11.44**	**138.1**	3.44	**63.0**	3.98	1.48	4.92	**134**	12.4	**87.3**
ABG	**10.7**	**8.16**	1.87	**126.5**	**54.9**	12.01	4.31	3.49	1.78	**83.7**	**135**	13.2
BCG	1.61	**6.98**	**5.52**	11.25	**121.0**	**125.2**	1.56	3.42	3.05	11.3	**110**	**123**
CAG	**10.1**	1.62	**11.51**	**113.6**	10.46	**128.9**	4.01	1.52	4.79	**134**	12.2	**86.7**
ABCG	**15.1**	**8.7**	**10.35**	**129.1**	**129.1**	**129.5**	5.53	3.75	4.504	**108.1**	**108.5**	**108.2**

5. DISCUSSION

Fault detection and classification in UPFC integrated transmission line using single terminal based DWT is proposed. From the above results it is observed that the scheme works fine in all the different variation of system parameters such as Rf, SI, FIA, phase reversal, fault location and UPFC condition. From the Figure 2 to Figure 7, it is clearly noticed that the fault is detected and classified within a cycle of time period (20ms). Table 1 to Table 7 presents the respective fault detection time (FDT) at different distance of fault occurrence under different types of fault and the fault classification. Table 8 presents a comparision study of spectral energy of different types of fault occurs before UPFC and after UPFC. The proposed scheme result has been compared to the existing wavelet entropy based scheme [28]. From this table it is noticed that the consideration of absolute entropy coefficient values from the literature [28] is found to be very high in the order of 10^5 (In AG fault 2.82x 10^5 for A-phase, 1.92x 10^5 for B-phase and 1.83x 10^5 for C-phase before UPFC) before UPFC and after UPFC condition compared to the proposed scheme shown in red numerical value (In AG fault 129.6 for A-phase, 34.87 for B-phase and 3.41 for C-phase before UPFC).

If the absolute coefficient value is very high in the order of 10^5 then the processing time for fault detection requires high to detect the fault as a result of which the relay will take more time to detect the fault which affects the reliability and security of the costly equipment and is not acceptable in the relaying scheme. For this reason authors in the literature [28] are unable to address the fault detection time. However the proposed scheme clearly address the fault detection time by considering different parameters of transmission line and UPFC condition in Table 1 to Table 8 and it is found that in all situation the fault detection time remains within a cycle period of time (20ms). Further the bold red numerical value of Table 8 shows the value of spectral energy content of each phase before UPFC and after UPFC respectively.The numerical value more than threshold (Th=25) indicates the fault in that phase and the numerical value which is less than threshold (Th=25) indicates the healthy phase. All the spectral energy value of each phase are considered at a

sample after the incidence of fault. Therefore the proposed scheme is very effective, accurate and simple to detect the fault with minimum fault detection time to classify the fault.

6. CONCLUSION

Fault detection and classification in a UPFC integrated transmission line using single terminal based DWT is proposed. The scheme of spectral energy based one terminal including UPFC using DWT has been successfully tested in matlab 2010A simulation under the variation of different system parameters such as *Rf, SI, FIA,* phase reversal and UPFC operating condition V_{se} and θ_{se}. It is observed that the scheme works fine in all such variation to detect and classify the fault. Futher the fault detection time to detect the fault remains within a cycle period of time (20ms). The proposed scheme has been compared to the existing scheme and found to be effective to detect the fault within 20ms time. Therefore the proposed system of SE based one terminal scheme is very effective as it is less sensitive to synchronization error as compared to the time domain of differential current scheme.

REFERENCES

[1] N. G. Hingorani and L. Gyugyi, Understanding FACTS Concepts and Technology of Flexible AC Transmission Systems, New York: IEEE Press, 2000.

[2] S. R. Samantaray. "A Data-Mining Model for Protection of FACTS-Based Transmission Line", in *IEEE Transactions on Power Delivery*, 2013; 28(2): 612-618.

[3] L.N. Tripathy, M. K. Jena, S. R Samantray. "Differential relaying scheme for tapped transmission line connecting UPFC and wind farm", *International Journal of Electrical Power & Energy Systems*, 2014; 60 (2): 245-257.

[4] L.N. Tripathy, S.R Samantray, P.K Dash. "A fast time–frequency transform based differential relaying scheme for UPFC based double-circuit transmission line", *International Journal of Electrical and Power Energy system,* 2016; 77(1): 404-417.

[5] Zhou X, Wang H, R.K Agarwal, P. Beaumont. "Performance of evaluation of distance relay as applied to a transmission system with UPFC", *IEEE Transaction on Power Delivery*, 2006; 21(3): 1137-1147.

[6] M.H.J. Boolen. "Traveling wave based protection of double circuit lines", *Proceedings of Institute of Electrical and Electronics Engineers C- Generation, Transmission and Distribution,* 1993*;* 140 (2): 37–47.

[7] SONG Y.H, A.T Johns, Q. Y. Xuan. "Artificial neural network based protection scheme for controllable series compensated EHV transmission lines", *IEE Proceeding on Generation, Transmission & Distribution*, 1996; 143(1): 535–540.

[8] P.K. Dash, A. K Pradhan, G. Panda. "A novel fuzzy neural network based distance relaying scheme", *IEEE Transaction on Power Delivery,* 2000; 15(3): 902–907.

[9] M. Chamia, S. Liberman. "Ultra high speed relay for EHV/UHV transmission lines", *IEEE Transactions on Power Apparatus and Systems,* 1978; 97(6): 2104-2112.

[10] S. R. Samantaray, P. K. Dash. "High impedance fault detection in distribution feeders using extended kalman filter and support vector machine", *European Transaction on Electrical Power,* 2010; 20(3): 382-393.

[11] V. L. Pham, K. P. Wong. "Wavelet transform based algorithm for harmonic analysis of power system waveform", *proceeding on Institutionof Electrical Engineering, Generation, Transmission and Distribution,* 1999; 146(3): 249–254.

[12] M. F. Habban, M. Manap, A.R. Abdullah, M.H. Jopri, T. Sutikno. "An Evaluation of linear time frequency distribution Analysis for VSI switch faults identification", *International Journal of Power Electronics and Drive system,* 2017; 8(1): 1-9.

[13] S. Azimi and M.V. Amiri. "Concurrent Detection and Classification of faults in Matrix Converter using Trans-conductance", *International Journal of Power Electronics and Drive system,* 2014; 5(1): 93-100.

[14] S. Dhara, A. K. Shrivastav, P. K. Sadhu, A. Ganguly. "A fault current limiter circuit to improve transient stability in power system", *International Journal of Power Electronics and Drive system*, 2016; 7(3): 769-780.

[15] Y. S Rao, G. Ravi Kumar, G. Keshab Rao. "A new approach for classification of fault in transmission line with combination of wavelet multi resolution analysis and neural networks", *International Journal of Power Electronics and Drive system,* 2017; 8(1): 505-512.

[16] S. K. Mishra, L.N Tripathy, S.C Swain. "An Adaline LMS control and DWT approach based differential relaying STATCOM integrated line", *International Journal of Control Theory and Applications*, 2017; 10 (37): 281-296.

[17] S. K. Mishra, L. N Tripathy, S.C Swain. "The Detection & Classification of fault in a SVC integrated Double circuit Transmission line using FDST", *International Journal of Control Theory and Applications*, 2017; 10 (37): 241-255.

[18] M. K. Jena, S. R. samantray, L. N. tripathy. "Decision tree-induced fuzzy rule-based differential relaying for transmission line including unified power flow controller and wind-farms", in *IET Generation, Transmission and Distribution*, 2014; 8 (12): 2144-2152.

[19] Ribeiro, P.F. "*Wavelet transform: an advanced tool for analyzing non-stationary harmonic distortions in power systems*", The IEEE International Conference on Harmonics in power systems, Bologna, Italy, 1994**.**

[20] S. MalIat. "A theory for multi-resolution signal decomposition: the wavelet representation", *IEEE Transaction on Pattern Analysis and Machine Intelligence*, 1989; 11(7): 674-693.
[21] W. K. Ngui, M. S. Leong, L.M. Hee, A. M. Abdelrhman "Mother wavelet Selection Method", *Applied Mechanics and Materials*, 2013;393(1): 953-958.
[22] Daubechies I, "Wavelet transform, time-frequency localization and signal analysis", *IEEE Transaction on Information Theory*, 1990; 36(5): 961-1005.
[23] H. A. Darwish, A. M. I. Talab, a.H Osman, N. M Mansur, O. P. Mallik. "*Spectral energy differential approach for transmission line protection*", proceeding on PSCE, Atlanta: USA, 2006: 1931–1937
[24] L.N. Tripathy, M. K. jena, S. R Samantray. "Differential relaying scheme for tapped transmission line connecting UPFC and wind farm", *International Journal of Electrical Power & Energy Systems*, 2014; 60 (2): 245-257
[25] L.N. Tripathy, S.R Samantray, P.K Dash. "Sparse S-transform for location of faults on transmission lines operating with unified power flow controller", in *IET Generation, Transmission & Distribution*, 2015; 9(15): 2108-2116
[26] A. Yadav, A. Swetapadma. "A single ended directional fault section identifier and fault locator for double circuit transmission lines using combined wavelet and ANN approach", *International Journal of Electrical Power & Energy Systems*, 2015; 69 : 27-33.
[27] W. Elmore, Protective Relaying Theory and Applications, second ed., Marcel Dekker, Inc., New York, 2005.
[28] El-Zonkoly and H. Desouki, "Wavelet Entropy Based Algorithm for Fault Detection and Classification in FACTS Compensated Transmission Line," *Energy and Power Engineering*, 2011; 33 (8): 1368-1374.